

# Reactivity Control in Iron(III) Amino Triphenolate Complexes: Comparison of Monomeric and Dimeric Complexes

Christopher J. Whiteoak,<sup>†</sup> Blerina Gjoka,<sup>‡</sup> Eddy Martin,<sup>†</sup> Marta Martínez Belmonte,<sup>†</sup> Eduardo C. Escudero-Adán,<sup>†</sup> Cristiano Zonta,<sup>‡</sup> Giulia Licini,<sup>\*,‡</sup> and Arjan. W. Kleij<sup>\*,†,§</sup>

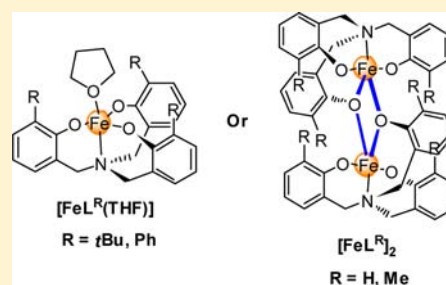
<sup>†</sup>Institute of Chemical Research of Catalonia (ICIQ), Av. Països Catalans 16, 43007 Tarragona, Spain

<sup>‡</sup>Dipartimento di Scienze Chimiche, Università di Padova, Via Marzolo 1, 35131, Padova, Italy

<sup>§</sup>Catalan Institute of Research and Advanced Studies (ICREA), Pg. Lluís Companys 23, 08010 Barcelona, Spain

## S Supporting Information

**ABSTRACT:** Iron(III) amino triphenolate complexes with different substituents in the *ortho*-position of the phenolate moiety (R = H, Me, *t*Bu, or Ph) have been synthesized by the reaction of iron(III) chloride and the sodium salt (Na<sub>3</sub>L<sup>R</sup>) of the requisite ligand. The complexes have been shown to be of either monomeric ([FeL<sup>R</sup>(THF)]) or dimeric ([FeL<sup>R</sup>]<sub>2</sub>) nature by a combination of X-ray diffraction, <sup>1</sup>H NMR, solution magnetic susceptibility, and cyclic voltammetry studies. These analytical studies have shown that the monomeric and dimeric [FeL<sup>R</sup>] complexes behave distinctively, and that the dimer stability is a function of the *ortho*-positioned groups. Both the dimeric as well as monomeric complexes were tested as catalysts for the catalytic cycloaddition of carbon dioxide to oxiranes, and the data show that the monomeric complexes are able to mediate this conversion with significantly higher activities than the dimeric complexes. This difference in reactivity is controlled by the substitution pattern on the ligand L<sup>R</sup>, and is in line with the catalytic requisite of binding of the epoxide substrate by the iron(III) center.



## INTRODUCTION

Iron mediated catalysis has and continues to receive considerable attention as a result of the relatively low toxicity and price of iron when compared to late transition metals.<sup>1–4</sup> In addition, iron is one of the most abundant metals in nature and plays a key role in many essential enzymatic conversions,<sup>5</sup> which continues to inspire the use of iron in synthetic catalysis. Simple iron salts have been shown to be capable of mediating some catalytic conversions, for example, in Fenton chemistry.<sup>6</sup> To attain greater control of the products and increase activities, ligand systems are generally included in synthetic catalysts. The ligands present in these synthetic catalysts significantly affect reactivity by a combination of electronic and steric effects.

Recently, a tripodal ligand system bearing a central amino donor and three phenoxide donors (NO<sub>3</sub> donor ligand) has attracted great interest (amino triphenol, Figure 1).<sup>7</sup> We consider this ligand to be a combination of the well exploited N<sub>2</sub>O<sub>2</sub> donor ligand, *bis*-aminophenolate (salan) and the NPy<sub>3</sub> donor ligand, tripyridyl amine (TPA) (Figure 1), which have both given rise to a variety of metal complexes with interesting catalytic properties.<sup>8–15</sup> A major drawback of the salan ligand is its ability to form three principal ligand topologies around the metal center when the complex adopts an octahedral coordination mode; *cis*- $\alpha$ , *cis*- $\beta$ , and *trans* (Figure 1), and this results in limited potential for asymmetric catalysis compared with the corresponding more rigid Schiff bases.<sup>16</sup> Further, it is likely that these different ligand topologies will impart distinct

differences in activity and selectivity during catalysis. A representative example in iron catalysis of these differences in activities for different ligand topologies has been reported using an iron(II) *bis*-aminopyridyl complex (N<sub>2</sub>Py<sub>2</sub> donor ligand), where it has been shown that for oxidation catalysis the *cis*- $\alpha$  ligand topology leads to the most active catalyst over the *cis*- $\beta$  and *trans* topologies.<sup>17</sup> The amino triphenol ligand offers similar donor moieties to the salan ligand, with the benefit of a controlled coordination topology similar to the TPA ligand and to this end there have also been reports of “intermediate” NPy<sub>2</sub>O and NPyO<sub>2</sub> type donor ligands.<sup>18–24</sup> Another interesting advantage of the NO<sub>3</sub> donor ligand over the other types mentioned above, is the potential to realize neutral M(III) complexes.

With regards to catalytic activity, there have been relatively limited studies with metal complexes bearing the amino triphenol ligand. It has been reported that amino triphenolate complexes of titanium, zirconium and hafnium are active catalysts for lactide polymerization.<sup>25–27</sup> Efficient oxidation catalysis results have also been achieved using titanium, vanadium and molybdenum amino triphenolate complexes.<sup>28–30</sup> Iron(III) complexes bearing amino triphenolate ligands were originally reported by Koch and co-workers more than 10 years ago, but the catalytic potential of these complexes

Received: April 27, 2012

Published: September 24, 2012

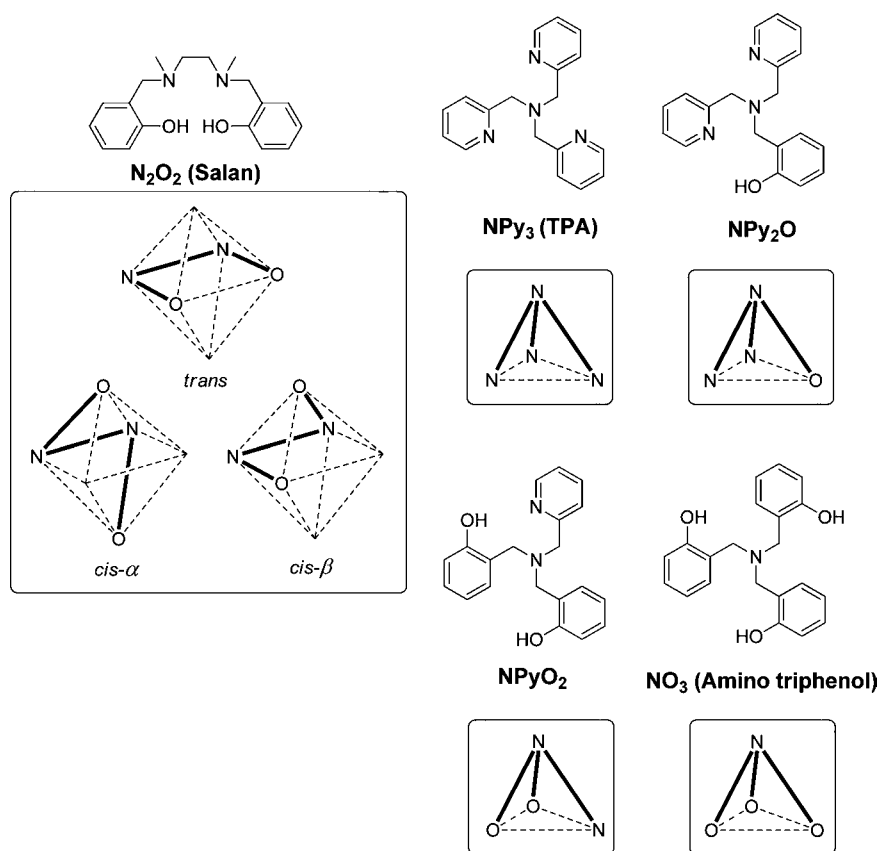


**Figure 1.** Structures of amino phenol, amino pyridyl phenol, and amino pyridyl ligands with representations of the possible ligand topologies adopted upon coordination to a metal.

was not exploited at the time.<sup>31</sup> More recently we have demonstrated that an iron(III) amino triphenolate complex is able to catalyze the cycloaddition of carbon dioxide to a wide variety of oxiranes and oxetanes to yield the corresponding cyclic carbonate products under energetically favorable reaction conditions, further demonstrating the applicability of these amino triphenol ligands.<sup>32</sup> Herein we will describe an extension of our previously reported work with respect to a refinement of the ligand structure by steric variation at the *ortho*-position of the phenoxide moiety (H, Me, *t*Bu, and Ph). The work will show characterization of these complexes by X-ray diffraction, cyclic voltammetry, <sup>1</sup>H NMR studies, and in addition, the reactivity of the complexes will be evaluated in terms of their ability to mediate the catalytic cycloaddition of carbon dioxide to oxiranes.

## EXPERIMENTAL SECTION

**General Procedures.** The ligands,  $H_3L^H$ ,  $H_3L^{Me}$ ,  $H_3L^{tBu}$ , and  $H_3L^{Ph}$  were prepared by known literature procedures.<sup>33</sup> The *mono*- and *di*-[iron(III) amino triphenolate] complexes were prepared using standard Schlenk and glovebox techniques under a nitrogen atmosphere. Once prepared, the complexes were no longer considered as air/moisture sensitive and were stored on the bench. Tetrahydrofuran used during the synthesis of the complexes was dried using a Solvent Purification System (SPS), and all other solvents were of reagent grade and used without any further purification. All other reagents and carbon dioxide (purchased from PRAXAIR) were used as received with no further purification. Elemental analysis was performed by the Unidad de Análisis Elemental at the Universidad de Santiago de Compostela (Spain). X-ray diffraction studies and mass spectroscopy measurements were carried out by the Research Support Group at ICIQ. FT-IR measurements were carried out on a Bruker

Optics FTIR Alpha spectrometer equipped with a DTGS detector, KBr beamsplitter at  $4\text{ cm}^{-1}$  resolution. UV-vis measurements were carried out on a Shimadzu UV-1800 spectrophotometer.

**[Fe<sup>L<sup>H</sup>]</sup>**<sub>2</sub>. To a suspension of sodium hydride (75.2 mg, 3.13 mmol) in tetrahydrofuran (10 mL) was slowly added a solution of  $H_3L^H$  (350 mg, 1.04 mmol) in tetrahydrofuran (10 mL). The mixture was stirred for 18 h and after this time it was added to a solution of anhydrous iron(III) chloride (167.7 mg, 1.04 mmol) in tetrahydrofuran (10 mL). The mixture was stirred for a further 4 h and then filtered through a path of Celite, followed by removal of the solvent to yield a brown residue, which was subsequently dissolved in dichloromethane, filtered and the solvent then removed to yield a brown powder. Yield: 397 mg (88%). Anal. Calcd for  $C_{42}H_{36}Fe_2N_2O_6$ : C, 64.97, H, 4.67; N, 3.61. Found: C, 64.92; H, 4.61; N, 3.38. MALDI(+)-MS (pyrene):  $m/z = 388 [M]^+$  (calcd. 388), 777  $[2M+H]^+$  (calcd. 777). UV-vis ( $CH_2Cl_2$ , 0.1 mM, 25 °C,  $\epsilon = L \cdot mol^{-1} \cdot cm^{-1}$ ): 314 nm ( $\epsilon = 7970$ ), 358 nm ( $\epsilon = 5290$ , sh), 430 nm ( $\epsilon = 3510$ ). Magnetic moment (298 K)  $\mu_{eff} = 4.14 \mu_B$ . The remaining complexes were prepared by using the same methodology.

**[Fe<sup>L<sup>Me</sup>]</sup>**<sub>2</sub>. Yield: 231 mg (89%). Anal. Calcd for  $C_{48}H_{48}Fe_2N_2O_6$ : C, 66.99; H, 5.62; N, 3.26. Found: C, 67.21; H, 5.82; N, 3.02. MALDI(+)-MS (pyrene):  $m/z = 430 [M]^+$  (calcd. 430). UV-vis ( $CH_2Cl_2$ , 0.1 mM, 25 °C,  $\epsilon = L \cdot mol^{-1} \cdot cm^{-1}$ ): 329 nm ( $\epsilon = 4065$ ), 416 nm ( $\epsilon = 3625$ ). Magnetic moment (298 K)  $\mu_{eff} = 6.74 \mu_B$ .

**[Fe<sup>L<sup>tBu</sup>(THF)]</sup>**. Yield: 408 mg (90%). Anal. Calcd for  $C_{37}H_{50}FeNO_4$ : C, 70.69; H, 8.02; N, 2.23. Found: C, 70.60; H, 8.34; N, 2.12. MALDI(+)-MS (dithranol):  $m/z = 557 [M+H-THF]^+$  (calcd. 557). UV-vis ( $CH_2Cl_2$ , 0.2 mM, 25 °C,  $\epsilon = L \cdot mol^{-1} \cdot cm^{-1}$ ): 329 nm ( $\epsilon = 3570$ ), 410 nm ( $\epsilon = 3135$ ). Magnetic moment (298 K)  $\mu_{eff} = 5.49 \mu_B$ .

**[Fe<sup>L<sup>Ph</sup>(THF)]</sup>**. Yield: 266 mg (61%). Anal. Calcd for  $C_{43}H_{38}FeNO_4$ : C, 75.00; H, 5.56; N, 2.03. Found: C, 74.75; H, 5.80; N, 2.12. MALDI(+)-MS (pyrene):  $m/z = 616 [M-THF]^+$  (calcd. 616). UV-vis ( $CH_2Cl_2$ , 0.2 mM, 25 °C,  $\epsilon = L \cdot mol^{-1} \cdot cm^{-1}$ ): 357 nm ( $\epsilon = 5460$ ), 426 nm ( $\epsilon = 5045$ ). Magnetic moment (298 K)  $\mu_{eff} = 5.53 \mu_B$ .

Table 1. X-ray Structure Data Collection and Refinement Parameters for All Reported Structures

	[FeL <sup>H</sup> ] <sub>2</sub>	[FeL <sup>Me</sup> (THF)]	[FeL <sup>tBu</sup> (H <sub>2</sub> O)]	[FeL <sup>Ph</sup> (THF)]	[FeL <sup>Ph</sup> (Py)]	[FeL <sup>Ph</sup> ( <i>trans</i> -2,3-epoxybutane)]
formula	C <sub>105</sub> H <sub>96</sub> Fe <sub>4</sub> N <sub>4</sub> O <sub>2</sub>	C <sub>28</sub> H <sub>32</sub> FeNO <sub>4</sub>	C <sub>33</sub> H <sub>46</sub> FeNO <sub>5</sub>	C <sub>43</sub> H <sub>34</sub> FeNO <sub>4</sub>	C <sub>44</sub> H <sub>35</sub> FeN <sub>2</sub> O <sub>3</sub>	C <sub>43</sub> H <sub>38</sub> FeNO <sub>4</sub>
Fw (g·mol <sup>-1</sup> )	1829.26	502.40	592.56	684.56	695.59	688.59
T (K)	100(2)	100(2)	100(2)	100(2)	100(2)	100(2)
λ (Å)	0.71073	0.71073	0.71073	0.71073	0.71073	0.71073
crystal system	triclinic	triclinic	monoclinic	monoclinic	monoclinic	monoclinic
space group	P $\bar{1}$	P $\bar{1}$	C2/c	P2 <sub>1</sub> /c	P2 <sub>1</sub> /c	P2 <sub>1</sub> /c
a (Å)	13.5240(13)	10.4445(6)	25.102(2)	16.0348(19)	16.140(2)	16.0716(16)
b (Å)	17.1679(17)	10.9051(6)	10.9015(11)	16.1658(18)	16.580(2)	16.2018(17)
c (Å)	19.236(2)	11.2722(6)	25.252(3)	13.0742(14)	12.8255(16)	13.2037(12)
α (deg)	77.392(3)	73.886(2)	90.00	90.00	90.00	90.00
β (deg)	79.290(3)	75.873(2)	112.938(3)	92.126(4)	91.774(4)	94.218(3)
γ (deg)	78.116(4)	79.199(2)	90.00	90.00	90.00	90.00
volume (Å <sup>3</sup> ), Z	4218.4(7), 2	1186.23(11), 2	6363.8(11), 8	3386.7(7), 4	3430.3(8), 4	3428.8(6), 4
ρ(calcd) (mg·m <sup>-3</sup> )	1.440	1.407	1.237	1.343	1.347	1.334
μ (mm <sup>-1</sup> )	0.744	0.671	0.513	0.491	0.484	0.485
absorption correction	empirical	empirical	empirical	empirical	empirical	empirical
refinement method	full-matrix least-squares on F <sup>2</sup>	full-matrix least-squares on F <sup>2</sup>	full-matrix least-squares on F <sup>2</sup>	full-matrix least-squares on F <sup>2</sup>	full-matrix least-squares on F <sup>2</sup>	full-matrix least-squares on F <sup>2</sup>
data/restraints/parameters	26557/0/1129	6294/0/311	5817/4/382	8248/641/586	8392/204/496	8457/2746/953
GOF on F <sup>2</sup>	1.043	1.041	1.161	1.066	1.050	1.056
final R indices [I > 2σ(I)]	R <sub>1</sub> = 0.0546	R <sub>1</sub> = 0.0359	R <sub>1</sub> = 0.0833	R <sub>1</sub> = 0.0979	R <sub>1</sub> = 0.0770	R <sub>1</sub> = 0.0678
	wR <sub>2</sub> = 0.1238	wR <sub>2</sub> = 0.0944	wR <sub>2</sub> = 0.2054	wR <sub>2</sub> = 0.2416	wR <sub>2</sub> = 0.1640	wR <sub>2</sub> = 0.1624
R indices (all data)	R <sub>1</sub> = 0.1003	R <sub>1</sub> = 0.0402	R <sub>1</sub> = 0.1002	R <sub>1</sub> = 0.1453	R <sub>1</sub> = 0.1346	R <sub>1</sub> = 0.0944
	wR <sub>2</sub> = 0.1438	wR <sub>2</sub> = 0.0970	wR <sub>2</sub> = 0.2144	wR <sub>2</sub> = 0.2524	wR <sub>2</sub> = 0.1824	wR <sub>2</sub> = 0.1769
largest diff. peak and hole (e Å <sup>-3</sup> )	0.833 and -0.889	0.822 and -0.257	1.267 and -0.671	1.161 and -1.170	0.426 and -1.032	0.798 and -0.972

**Catalytic Experiments.** In a typical catalytic experiment the oxirane substrate (2.0 mmol), tetra-butyl-ammonium bromide (32.6 mg, 0.1 mmol), the respective iron(III) amino triphenolate complex (0.01 mmol of complex [FeL<sup>H</sup>]<sub>2</sub> or [FeL<sup>Me</sup>]<sub>2</sub>, and 0.02 mmol [FeL<sup>tBu</sup>(THF)] or [FeL<sup>Ph</sup>(THF)]) and mesitylene (278 μL, 2.0 mmol) were dissolved in the respective solvent (5 mL). The reaction mixture was then transferred to a stainless steel autoclave and three cycles of pressurization and depressurization with carbon dioxide were applied (*p*CO<sub>2</sub> = 0.5 MPa). The final pressure was then adjusted to 1.0 MPa, and the reaction was left stirring at the required temperature for 18 h. After this time, the yield was calculated using the <sup>1</sup>H NMR spectrum (*d*<sub>6</sub>-DMSO) of an aliquot of the reaction mixture and mesitylene as the internal standard.

**Magnetic Susceptibility Measurements.** Evans NMR technique was used for the determination of the magnetic susceptibilities of the complexes.<sup>34,35</sup> The solvent system used was CDCl<sub>3</sub>:cyclohexane (95:5 v/v), and the diamagnetic susceptibility was neglected during the calculation. To each of the samples, pyridine was added to give 10% v/v of the solvent system where the magnetic susceptibility in the presence of pyridine is reported.

**UV-vis Titration Studies.** A 0.1 mM dichloromethane solution of [FeL<sup>H</sup>]<sub>2</sub> was prepared and the UV-vis spectrum recorded at 25 °C using a quartz cell with a 1 cm path length. This solution was titrated with propylene oxide or pyridine, with the UV-vis spectrum measured immediately after each addition.

**Cyclic Voltammetry Studies.** Cyclic voltammetric measurements were carried out with a Princeton Applied Research PARSTAT 2273 electrochemical analyzer. A three electrode assembly, comprising a glassy carbon working electrode, a platinum wire auxiliary electrode, and Ag-AgCl (sat. NaCl) reference electrode was used. The experimental data were obtained under an argon atmosphere in dichloromethane solvent using NBu<sub>4</sub>PF<sub>6</sub> as supporting electrolyte. Results involving the presence of pyridine were obtained by using a dichloromethane:pyridine (90:10 v/v) solvent system.

**X-ray Crystallography.** Crystals suitable for single crystal X-ray analysis were obtained by slow evaporation of tetrahydrofuran solutions of [FeL<sup>Me</sup>(THF)], [FeL<sup>tBu</sup>(THF)], and [FeL<sup>Ph</sup>(THF)] or in the case of [FeL<sup>H</sup>]<sub>2</sub>, crystals were obtained from a concentrated toluene solution after three weeks. The structure obtained for [FeL<sup>tBu</sup>] contains a molecule of water instead of the expected molecule of tetrahydrofuran as the coligand and is denoted as [FeL<sup>tBu</sup>(H<sub>2</sub>O)]. The crystals of [FeL<sup>Ph</sup>(Py)] were grown by slow evaporation of a concentrated solution of the complex in tetrahydrofuran/pyridine (50:1) and the crystals of [FeL<sup>Ph</sup>(*trans*-2,3-epoxybutane)] were obtained in a similar manner from a solution of tetrahydrofuran/*trans*-2,3-epoxybutane (25:1).

The measured crystals were stable under atmospheric conditions; nevertheless they were treated under inert conditions immersed in perfluoropoly ether as protecting oil for manipulation. Data collection measurements were made on a Bruker-Nonius diffractometer equipped with an APPEX 2 4 K CCD area detector, an FR591 rotating anode with MoKα radiation, Montel mirrors, and a Kryoflex low temperature device (*T* = -173 °C). Full-sphere data collection was used with ω and φ scans. Programs used: data collection Apex2 V2011.3 (Bruker-Nonius 2008), data reduction Saint+ Version 7.60 A (Bruker AXS 2008) and absorption correction SADABS V. 2008-1 (2008). For structure solution SHELXTLVersion 6.10 (Sheldrick, 2000)<sup>36</sup> was used (Table 1). Structure refinement: SHELXTL-97-UNIX version.

## RESULTS AND DISCUSSION

**Complex Synthesis and Characterization.** Synthetic routes to all the ligands used in this investigation have been published previously, and the ligands have been synthesized as described in these reports.<sup>26</sup> The reaction of H<sub>3</sub>L<sup>R</sup> (R = H, methyl, *tert*-butyl, or phenyl) with 3 equiv of sodium hydride in tetrahydrofuran and subsequent addition of 1 equiv of iron(III) chloride yields analytically pure *mono*- or *di*-[iron(III)

Scheme 1. Synthesis of Mono- and Di-[Iron(III) Amino Triphenolate] Complexes

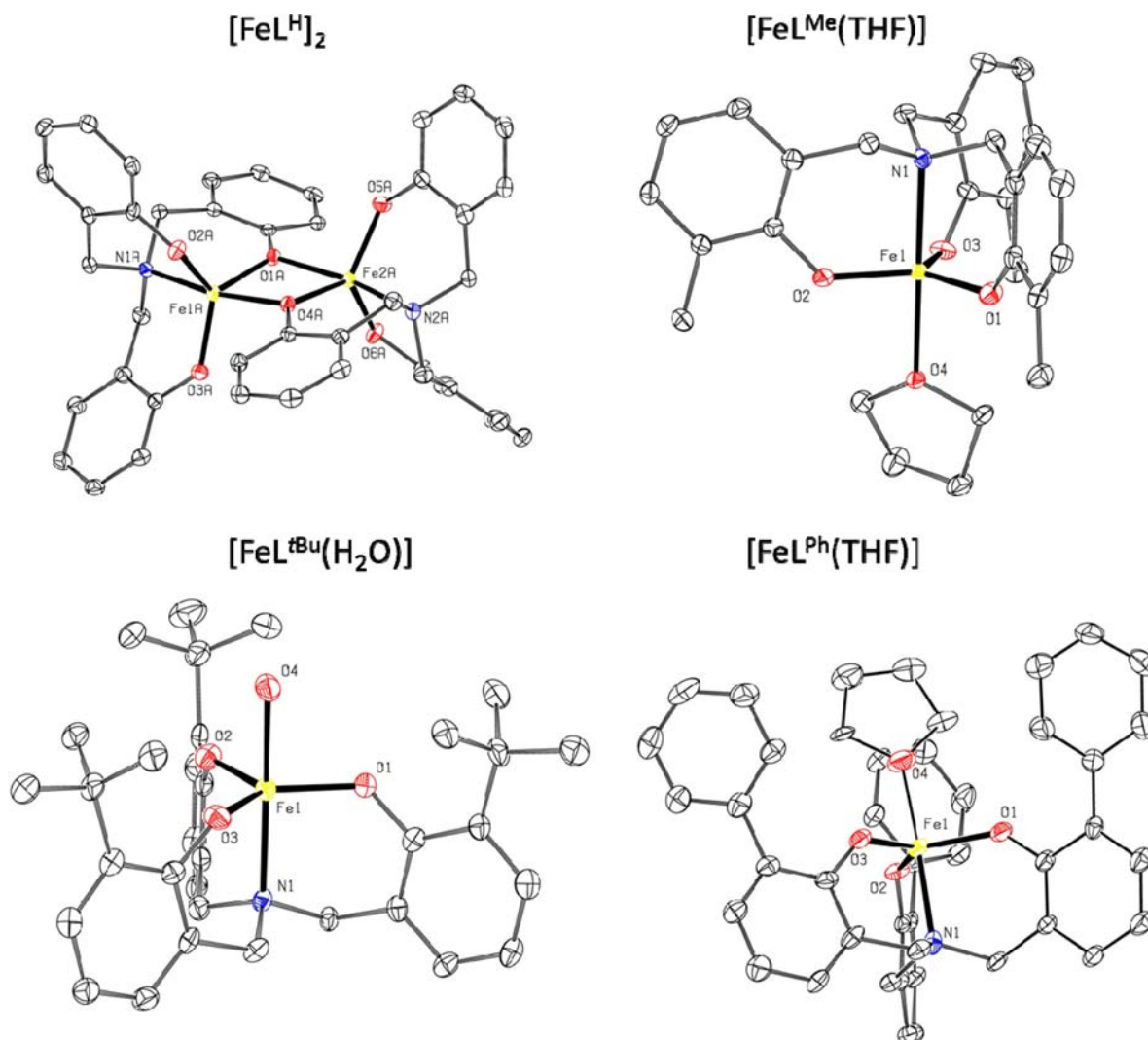
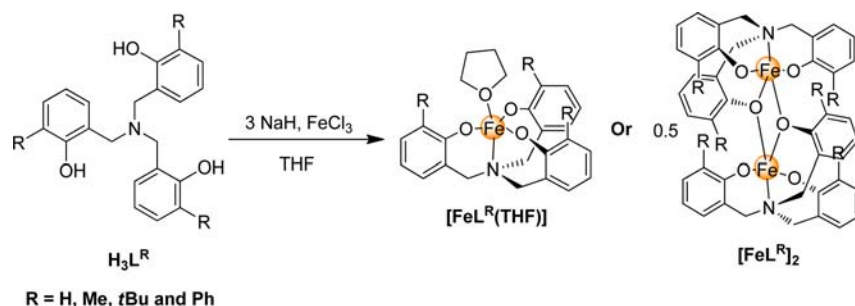


**Figure 2.** Solid state structures of  $[\text{FeL}^{\text{H}}]_2$  (top left),  $[\text{FeL}^{\text{Me}}(\text{THF})]$  (top right),  $[\text{FeL}^{\text{tBu}}(\text{H}_2\text{O})]$  (bottom left), and  $[\text{FeL}^{\text{Ph}}(\text{THF})]$  (bottom right). H-atoms, cocrystallized solvent and disorder have been omitted for clarity, and only a partial numbering scheme is provided.

amino triphenolate] complexes after filtration of the reaction mixture and removal of the solvent (Scheme 1). All complexes have been initially characterized by MALDI(+) mass spectrometry and elemental analysis, and the obtained data is consistent with the proposed structures. Further to this characterization data, it has been possible to obtain solid state structures of all the complexes, which confirm the presence of iron(III) amino triphenolate units.

**Solid State Structures.** Crystals suitable for X-ray diffraction studies were obtained by slow evaporation of

tetrahydrofuran solutions of the complexes, except for  $[\text{FeL}^{\text{H}}]_2$  where crystals were obtained from a concentrated toluene solution. The solid state structures of the complexes obtained are shown in Figure 2, with selected bond lengths and angles shown in Table 2. The molecular structure of the complex obtained from  $\text{H}_3\text{L}^{\text{H}}$  consists of two iron(III) amino triphenolate complexes forming a dimeric assembly,  $[\text{FeL}^{\text{H}}]_2$ , with one phenoxide O-atom from each individual complex acting as a bridging ligand, resulting in the formation of a central  $\text{Fe}_2\text{O}_2$  motif. The solid state structures of the complexes

Table 2. Selected Bond Lengths (Å) and Angles (deg) in [FeL<sup>H</sup>]<sub>2</sub>, [FeL<sup>Me</sup>(THF)], [FeL<sup>tBu</sup>(H<sub>2</sub>O)], and [FeL<sup>Ph</sup>(THF)]

	[FeL <sup>H</sup> ] <sub>2</sub>	[FeL <sup>Me</sup> (THF)]	[FeL <sup>tBu</sup> (H <sub>2</sub> O)]	[FeL <sup>Ph</sup> (THF)]
Bond Lengths (Å)				
Fe(1)–O(1)	1.9713(18)	1.8643(12)	1.885(4)	1.856(3)
Fe(1)–O(2)	1.8611(18)	1.8555(12)	1.853(4)	1.859(3)
Fe(1)–O(3)	1.8519(19)	1.8685(11)	1.861(4)	1.878(3)
Fe(1)–O(4)	2.0642(17)	2.1063(11)	2.097(4)	2.055(5)
Fe(1)–N(1)	2.1440(20)	2.1795(13)	2.178(4)	2.163(4)
Bond Angles (deg)				
O(1)–Fe(1)–O(2)	120.76(8)	121.15(5)	113.79(17)	116.22(14)
O(1)–Fe(1)–O(3)	116.00(8)	119.08(6)	130.41(17)	121.94(14)
O(2)–Fe(1)–O(3)	123.14(9)	119.58(5)	115.77(17)	121.82(14)
O(1)–Fe(1)–O(4)	77.44(7)	89.28(5)	92.16(16)	93.41(18)
O(1)–Fe(1)–N(1)	91.15(8)	91.71(5)	89.75(16)	90.11(13)
N(1)–Fe(1)–O(4)	168.33(8)	178.24(4)	172.98(17)	173.95(19)

obtained from H<sub>3</sub>L<sup>Me</sup>, H<sub>3</sub>L<sup>tBu</sup> and H<sub>3</sub>L<sup>Ph</sup> display complexes of a monomeric form containing an apical ligand originating from the solvent medium. The molecular structure obtained for recrystallized [FeL<sup>tBu</sup>(THF)] contains a water ligand in place of the expected tetrahydrofuran ligand, [FeL<sup>tBu</sup>(H<sub>2</sub>O)], which is likely to be a consequence of ligand exchange with water present in the solvent used during crystallization, promoted by the steric constraints imposed on the coordination sphere of the iron center by the bulky *tert*-butyl groups.

The molecular structure obtained for [FeL<sup>Me</sup>(THF)], as has been mentioned, shows the monomeric form of the complex, but further investigations (*vide infra*) indicate that a dimeric structure may be easily formed as in the case of [FeL<sup>H</sup>]<sub>2</sub>. We therefore propose that this complex forms a weak dimeric structure and that the crystals obtained are as a result of preferential crystallization of the monomer. No evidence of dimeric complexes in the cases of [FeL<sup>tBu</sup>(THF)] or [FeL<sup>Ph</sup>(THF)] are proposed.

The solid state structure of [FeL<sup>Me</sup>(THF)] displays idealized C<sub>3</sub> symmetry, with the angles between the oxygen atoms of the phenoxide moieties being 121.15(5)°, 119.08(6)°, and 119.58(5)° for O(1)–Fe(1)–O(2), O(1)–Fe(1)–O(3), and O(2)–Fe(1)–O(3), respectively. The corresponding angle between the amine and the oxygen atom of the tetrahydrofuran ligand (178.24(4)°) is close to the ideal value of 180° expected in a perfectly C<sub>3</sub> symmetrical molecule. The structure also displays similar bond length values for all the Fe–O bonds with the ligand and an elongated Fe–O bond length for the bond between the tetrahydrofuran and metal.

The addition of *tert*-butyl groups impacts severely on the C<sub>3</sub> symmetry of the complex in [FeL<sup>tBu</sup>(H<sub>2</sub>O)] compared with [FeL<sup>Me</sup>(THF)]. It appears that the *tert*-butyl groups have a significant steric effect on the structure. The angles between of O(1)–Fe(1)–O(2), O(1)–Fe(1)–O(3), and O(1)–Fe(1)–O(3) are significantly different from those expected in a perfect C<sub>3</sub> symmetrical molecule and have values of 113.79(17)°, 115.77(17)°, and 130.41(17)°, respectively. These distortions are similar in value to those observed by Safaei and co-workers for a similar complex containing a methanol ligand in the apical position.<sup>37</sup> A further difference in this molecule compared to [FeL<sup>Me</sup>(THF)] is that not all the Fe–O bond lengths between the metal and the ligand have the same length, with one of them being clearly elongated. The observation of these differences in structure adds weight to the proposal that the original tetrahydrofuran ligand has exchanged with the water ligand during crystallization to form a more stable complex.

Similar but less significant distortions from perfect C<sub>3</sub> symmetry are also observed in the case of [FeL<sup>Ph</sup>(THF)] compared with [FeL<sup>tBu</sup>(H<sub>2</sub>O)], indicating that the phenyl groups contribute less to the steric constraints immediately around the iron(III) center. The resulting angles being 116.22(14)°, 121.82(14)°, and 121.94(14)° for O(1)–Fe(1)–O(2), O(1)–Fe(1)–O(3), and O(1)–Fe(1)–O(3), respectively.

The dimeric complex, [FeL<sup>H</sup>]<sub>2</sub>, displays two Fe–O bonds with lengths of 1.8611(18) Å and 1.8519(19) Å corresponding to the nonbridging phenoxide moieties and two longer Fe–O bonds with lengths of 1.9713(18) Å and 2.0642(17) Å for the bonds involving the bridging phenoxide moieties. These bond lengths are similar to those previously reported for a similar dimeric structure.<sup>25</sup>

**Magnetic Susceptibility Measurements.** The Evans method was used to calculate the solution magnetic susceptibility values,  $\mu_{\text{eff}}$  for all complexes (Table 3).<sup>34,35</sup> In

Table 3. Solution Magnetic Susceptibility Data ( $\mu_{\text{eff}}$ ) for [FeL<sup>H</sup>]<sub>2</sub>, [FeL<sup>Me</sup>]<sub>2</sub>, [FeL<sup>tBu</sup>(THF)], and [FeL<sup>Ph</sup>(THF)]<sup>a,b</sup>

	complex	complex + pyridine
[FeL <sup>H</sup> ] <sub>2</sub>	2.12 $\mu_{\text{B}}$	5.72 $\mu_{\text{B}}$
[FeL <sup>Me</sup> ] <sub>2</sub>	3.37 $\mu_{\text{B}}$	5.43 $\mu_{\text{B}}$
[FeL <sup>tBu</sup> (THF)]	5.49 $\mu_{\text{B}}$	5.50 $\mu_{\text{B}}$
[FeL <sup>Ph</sup> (THF)]	5.53 $\mu_{\text{B}}$	5.95 $\mu_{\text{B}}$

<sup>a</sup>In CDCl<sub>3</sub> at 298 K. <sup>b</sup>Values are on a per iron atom basis.

addition to this we have also calculated the  $\mu_{\text{eff}}$  values for all the complexes in the presence of pyridine for comparison. Both [FeL<sup>tBu</sup>(THF)] and [FeL<sup>Ph</sup>(THF)] give rise to  $\mu_{\text{eff}}$  values consistent with those expected for high-spin iron(III) complexes ( $\mu_{\text{eff}} = 5.49 \mu_{\text{B}}$  and  $5.53 \mu_{\text{B}}$  respectively). In the presence of pyridine these complexes also display  $\mu_{\text{eff}}$  values consistent with high-spin iron(III) complexes ( $\mu_{\text{eff}} = 5.50 \mu_{\text{B}}$  and  $\mu_{\text{eff}} = 5.95 \mu_{\text{B}}$  respectively). We propose that in both these cases the iron(III) complexes are in the monomeric form, both before and after addition of pyridine.

Calculation of the  $\mu_{\text{eff}}$  values for the dimeric complexes [FeL<sup>H</sup>]<sub>2</sub> and [FeL<sup>Me</sup>]<sub>2</sub> gives rise to  $\mu_{\text{eff}}$  values which are lower than expected for noncoupled dimeric high-spin iron(III) complexes ( $\mu_{\text{eff}} = 2.12 \mu_{\text{B}}$  and  $3.37 \mu_{\text{B}}$  on a per iron atom basis, respectively). The decrease in the measured  $\mu_{\text{eff}}$  values of these complexes can be attributed to antiferromagnetic coupling between the two iron(III) atoms. Other antiferromagnetically coupled iron(III) phenolate bridged dimeric complexes have

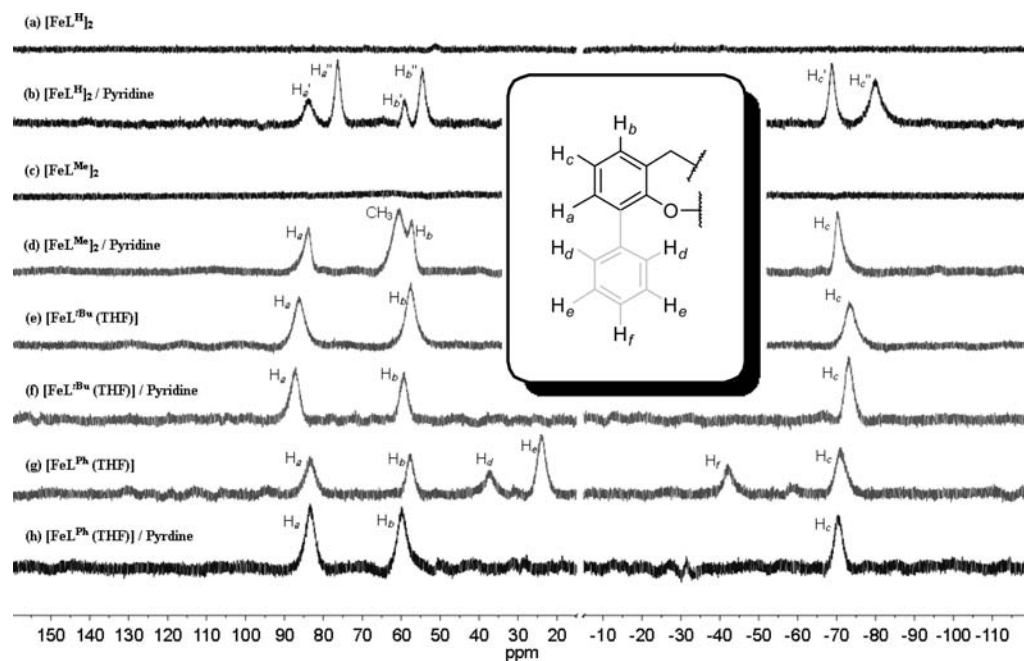
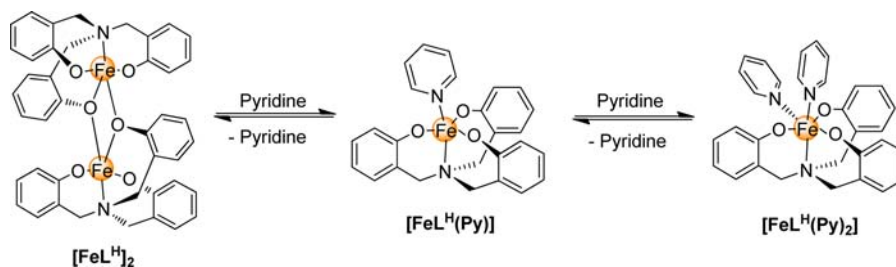


**Figure 3.**  $^1\text{H}$  NMR spectra (500 MHz,  $\text{CDCl}_3$ , 298 K) of  $[\text{FeL}^{\text{H}}]_2$ ,  $[\text{FeL}^{\text{Me}}]_2$ ,  $[\text{FeL}^{\text{tBu}}(\text{THF})]$ , and  $[\text{FeL}^{\text{Ph}}(\text{THF})]$ ; with/without the addition of  $d_5$ -Pyridine. For clarity 15 to  $-5$  ppm region omitted.

**Scheme 2. Schematic Representation of the Proposed Reaction of Pyridine with  $[\text{FeL}^{\text{H}}]_2$**



been reported previously and suppression of the  $\mu_{\text{eff}}$  value is observed as a result.<sup>38–41</sup> The values also imply that the antiferromagnetic coupling in  $[\text{FeL}^{\text{H}}]_2$  is significantly stronger than in  $[\text{FeL}^{\text{Me}}]_2$ , suggesting a stronger dimer in the former complex. Upon addition of pyridine to both of these dimeric complexes,  $\mu_{\text{eff}}$  values consistent with monomeric high-spin iron(III) complexes are obtained ( $\mu_{\text{eff}} = 5.72 \mu_{\text{B}}$  and  $5.43 \mu_{\text{B}}$  respectively).

**$^1\text{H}$  NMR Spectroscopy Studies.** Paramagnetic complexes generally exhibit broad resonances with large chemical shifts. The  $^1\text{H}$  NMR spectra of all the complexes were obtained in  $\text{CDCl}_3$  at 298 K and are shown in Figure 3, with the region between 15 and  $-5$  ppm omitted for clarity (this region principally displays resonances for the protio-impurities of the deuterated solvents, a broad resonance for the alkyl protons of the ligand and in the case of  $[\text{FeL}^{\text{tBu}}(\text{THF})]$ , a broad resonance for the protons of the *tert*-butyl group). Additionally, the  $^1\text{H}$  NMR spectra of all complexes have been obtained in a  $\text{CDCl}_3:d_5\text{-Pyridine}$  (90:10 v/v) mixture to allow for comparison with the species obtained in the solution magnetic susceptibility measurements. We have tentatively assigned the paramagnetically shifted resonances, as efforts to acquire 2D NMR spectra have proved to be unsuccessful.

In the  $^1\text{H}$  NMR spectra of both  $[\text{FeL}^{\text{H}}]_2$  and  $[\text{FeL}^{\text{Me}}]_2$ , there are no observable strongly shifted resonances to indicate the

presence of a paramagnetic species, most likely as a result of strong antiferromagnetic coupling between the two iron(III) centers resulting in very broad signals. Upon addition of pyridine to both of these complexes, it is possible to observe the appearance of new resonances in the 90 to  $-80$  ppm range, indicating the formation of paramagnetic species. In the case of  $[\text{FeL}^{\text{H}}]_2/\text{pyridine}$ , we propose that the observed resonances, shown in Figure 3, are those of the aromatic protons of the ligand. Three of the aromatic protons appear as a pair of resonances ( $H_{a'} = H_{a''}$ ,  $H_{b'} = H_{b''}$ , and  $H_{c'} = H_{c''}$ ), with the resonance corresponding to the remaining *ortho*-proton of the aromatic moiety being likely present in the 0–12 ppm range (see Supporting Information). We propose that a pair of resonances is observed for each proton because of the possibility of either one or two pyridine ligands coordinating to the iron(III) center, and this is further confirmed by the presence of only a single set of resonances when the experiment is run in neat  $d_5$ -pyridine (see Supporting Information). In the case of a single coordinated pyridine, the complex displays trigonal bipyramidal geometry, whereas upon coordination of a second pyridine ligand the complex becomes octahedral in geometry, resulting in different orbital overlap and therefore displaying slightly different chemical shifts (Scheme 2). The proposed ability of  $[\text{FeL}^{\text{H}}]_2$  to bind two external ligands and form an octahedral complex is a result of lower steric

constraints imposed by this ligand compared with the other ligand structures and this complex would also be similar in structure to the first iron(III) amino triphenolate complex reported by Koch and co-workers,  $[\text{FeL}^{\text{H}}(\text{bipy})]$ , containing a bipyridine ligand.<sup>31</sup> In the case of  $[\text{FeL}^{\text{Me}}]_2$ , the steric constraints imparted by the methyl groups of the ligand prevent the coordination of a second pyridine ligand, and hence only a single set of resonances ( $H_a$ ,  $H_b$ , and  $H_c$ ) are observed for each proton. The protons from the methyl group of  $[\text{FeL}^{\text{Me}}]_2$  are observed as the second resonance ( $\text{CH}_3$ ) at around 60 ppm.

Both the spectra of  $[\text{FeL}^{\text{tBu}}(\text{THF})]$  and  $[\text{FeL}^{\text{Ph}}(\text{THF})]$  display the paramagnetically shifted resonances for the aromatic protons ( $H_a$ ,  $H_b$ , and  $H_c$ ) in the absence of pyridine, further adding to the evidence that these two complexes exist in their monomeric form. Upon addition of pyridine to  $[\text{FeL}^{\text{tBu}}(\text{THF})]$  there is no change in the spectrum, as the pyridine is only substituting the tetrahydrofuran ligand to yield  $[\text{FeL}^{\text{tBu}}(\text{Py})]$  in situ. The same behavior is not true for  $[\text{FeL}^{\text{Ph}}(\text{THF})]$ , as after addition of pyridine the resonances which we propose are assigned to the protons of the *ortho*-phenyl group disappear ( $H_b$ ,  $H_v$ , and  $H_f$ ). The solid state structure of  $[\text{FeL}^{\text{Ph}}(\text{Py})]$  has been obtained (Figure 4, Table 4) and indicates that pyridine can coordinate and act as a ligand though resulting in a reduced rotational freedom of the Ph groups of the amino triphenolate ligand.

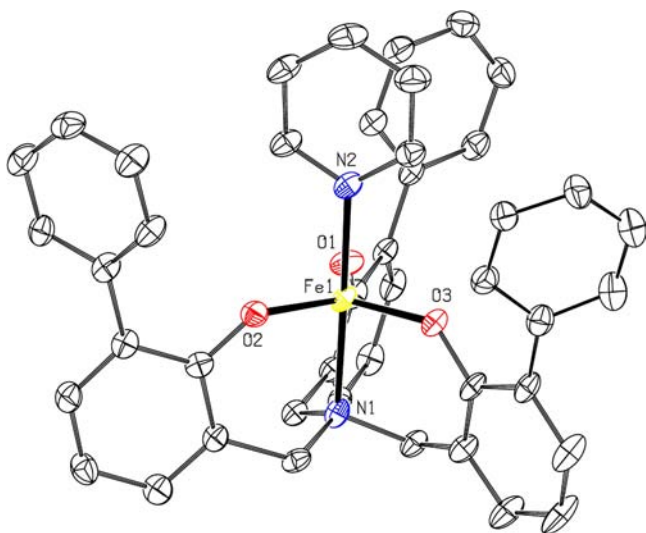


**Figure 4.** Solid state structure of  $[\text{FeL}^{\text{Ph}}(\text{Py})]$ . H-atoms and cocrystallized solvent molecules, and rotational disorder are omitted for clarity. A partial numbering scheme (around the Fe center) is provided.

**Table 4.** Selected Bond Lengths (Å) and Angles (deg) in  $[\text{FeL}^{\text{Ph}}(\text{Py})]$

bond lengths (Å)		bond angles (deg)	
Fe(1)–O(1)	1.856(3)	O(1)–Fe(1)–O(2)	123.40(14)
Fe(1)–O(2)	1.870(3)	O(1)–Fe(1)–O(3)	117.45(13)
Fe(1)–O(3)	1.860(3)	O(1)–Fe(1)–N(1)	88.43(13)
Fe(1)–N(1)	2.182(4)	O(1)–Fe(1)–N(2)	89.76(13)
Fe(1)–N(2)	2.135(4)	N(1)–Fe(1)–N(2)	177.99(13)

**UV–vis Studies.** The electronic spectra of all the complexes are very similar to one another (see the Supporting

Information). A ligand-to-metal charge transfer band (LMCT) is observed in all the complexes around 400–450 nm. A second LMCT band is observed for all complexes around 310–360 nm and in addition,  $[\text{FeL}^{\text{H}}]_2$  displays a third LMCT band in this region as a shoulder at 358 nm which is most likely as a result of the bridging phenoxide moieties.

It has been previously reported that a complex similar to  $[\text{FeL}^{\text{Me}}]_2$  can be disrupted by titration with propylene oxide (i.e., a substrate used in cycloaddition catalysis, *vide infra*).<sup>25</sup> All the complexes presented in this work have also been titrated in a similar fashion (see Supporting Information). Upon titrating  $[\text{FeL}^{\text{Me}}]_2$  with propylene oxide we also observed a similar change in spectrum suggesting disruption of a dimeric structure. Titration of the remaining complexes with the same titrant does not give rise to any significant changes in the spectra, and therefore we propose that this is a result of  $[\text{FeL}^{\text{tBu}}(\text{THF})]$  and  $[\text{FeL}^{\text{Ph}}(\text{THF})]$  already being in the monomeric forms and that propylene oxide is not a strong enough ligand to disrupt the dimeric structure of  $[\text{FeL}^{\text{H}}]_2$ . When the dimeric complex  $[\text{FeL}^{\text{H}}]_2$  is titrated with pyridine (a stronger competitive ligand), a significant change in spectra is observed (Figure 5). For comparison  $[\text{FeL}^{\text{Ph}}(\text{THF})]$  was also titrated with an excess of pyridine and in this case only a small change in spectrum was observed. It is therefore suggested that  $[\text{FeL}^{\text{H}}]_2$  forms a stronger dimeric structure than  $[\text{FeL}^{\text{Me}}]_2$  and as a result  $[\text{FeL}^{\text{H}}]_2$  requires a stronger ligand to disrupt its dimeric structure.

**Electrochemical Studies.** Cyclic voltammetry studies have been carried out in dichloromethane for all the complexes (Figure 6 and Table 5). Data has also been obtained for all complexes in dichloromethane with pyridine (10% v/v). The monomeric complexes  $[\text{FeL}^{\text{tBu}}(\text{THF})]$  and  $[\text{FeL}^{\text{Ph}}(\text{THF})]$  exhibit quasi-reversible waves at  $-1.008$  and  $-0.825$  V, respectively. Both of these complexes exhibit changes in  $E_{1/2}$  upon addition of pyridine, although the nature of these waves remains quasi-reversible.

Both  $[\text{FeL}^{\text{H}}]_2$  and  $[\text{FeL}^{\text{Me}}]_2$  give rise to a more complex electrochemical behavior. In the case of  $[\text{FeL}^{\text{Me}}]_2$ , it appears that there are two sequential reductions (i.e., addition of an electron to both iron(III) centers independently), as though the iron(III) centers are coupled; the antiferromagnetic coupling is not as strong as that observed in  $[\text{FeL}^{\text{H}}]_2$ . Upon addition of pyridine to  $[\text{FeL}^{\text{Me}}]_2$  only a single quasi-reversible wave is observed with a similar  $E_{1/2}$  to the monomeric pyridine containing species derived from  $[\text{FeL}^{\text{Ph}}(\text{THF})]$ . The dimeric complex  $[\text{FeL}^{\text{H}}]_2$  exhibits a single quasi-reversible wave at  $-0.288$  V. This value is significantly lower than for the monomeric species, most likely because upon addition of an electron the electron density is completely delocalized between two iron centers ( $\text{Fe}_2\text{O}_2$  motif) rather than a single one, making this reduction more facile. Upon addition of pyridine to  $[\text{FeL}^{\text{H}}]_2$  a complex cyclic voltammogram containing three quasi-reversible waves is obtained, and we propose that this results from a mixture of monomeric species having either one or two pyridines associated to the complex as was discussed previously in the  $^1\text{H}$  NMR study of this complex (Scheme 2).

**Catalytic Studies.** Previously, we reported that an iron(III) amino triphenolate complex was able to successfully mediate the catalytic cycloaddition of carbon dioxide to a range of oxiranes and oxetanes.<sup>25</sup> Having established that the substitution pattern on the amino triphenolate ligand L has a pronounced effect on the electrochemical, spectroscopic, and solid state features, we next examined the influence of the

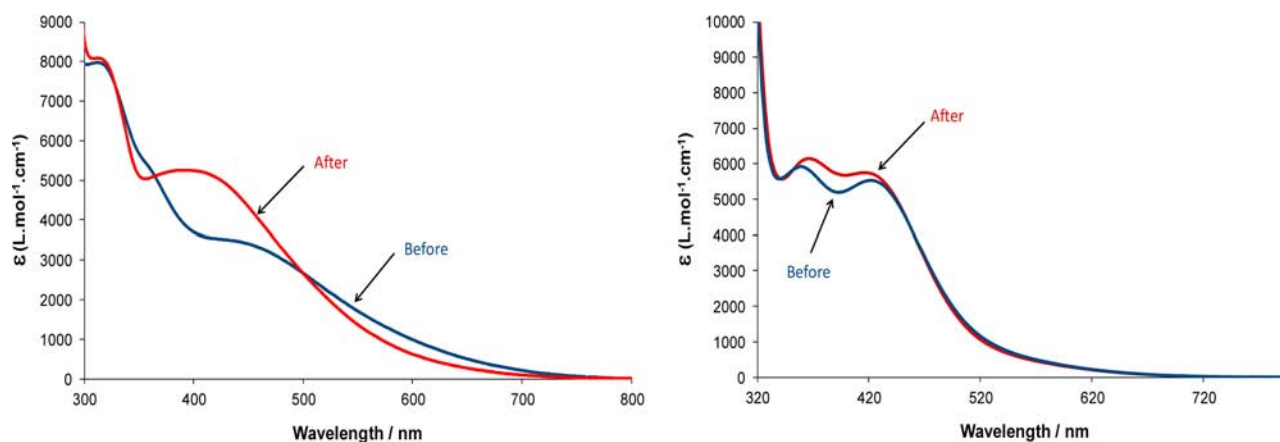


Figure 5. UV-vis spectra in DCM of  $[\text{FeL}^{\text{H}}]_2$  (left),  $[\text{FeL}^{\text{Ph}}(\text{THF})]$  (right), before and after addition of pyridine.

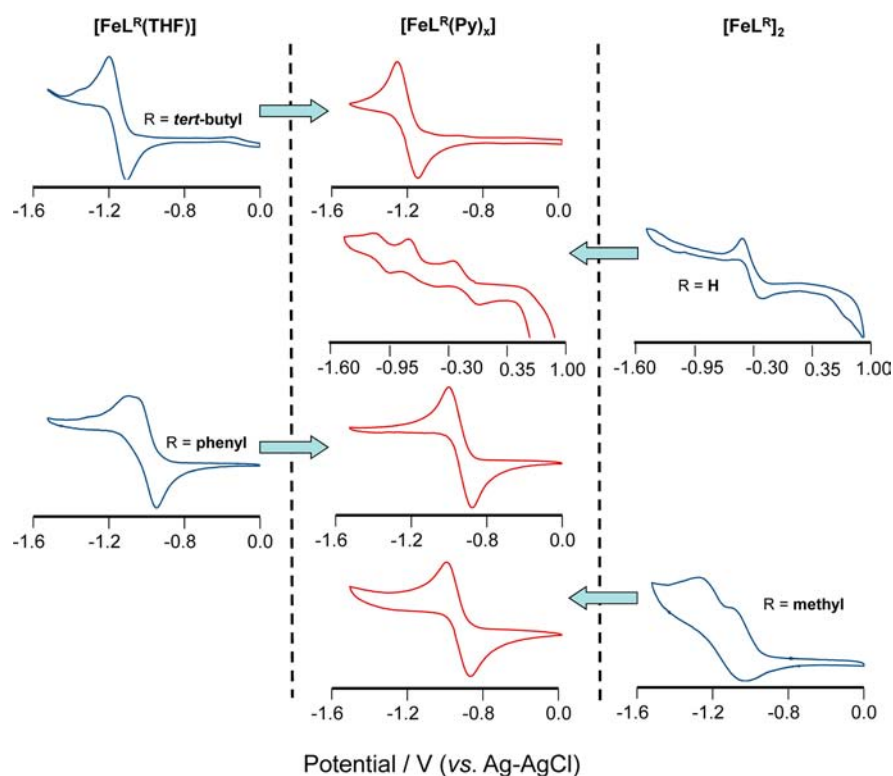


Figure 6. Cyclic voltammograms at 298 K in  $\text{CH}_2\text{Cl}_2$  at 298 K (scan rate =  $100 \text{ mV s}^{-1}$ ) using  $0.1 \text{ M NBu}_4\text{PF}_6$  as supporting electrolyte at a glassy carbon working electrode, platinum wire auxiliary electrode, and Ag-AgCl (sat. NaCl) reference electrode of  $[\text{FeL}^{\text{H}}]_2$ ,  $[\text{FeL}^{\text{Me}}]_2$ ,  $[\text{FeL}^{\text{tBu}}(\text{THF})]$ , and  $[\text{FeL}^{\text{Ph}}(\text{THF})]$ : before and after addition of 5% v/v pyridine.

Table 5. Electrochemical Data for  $[\text{FeL}^{\text{H}}]_2$ ,  $[\text{FeL}^{\text{Me}}]_2$ ,  $[\text{FeL}^{\text{tBu}}(\text{THF})]$ , and  $[\text{FeL}^{\text{Ph}}(\text{THF})]$ <sup>a</sup>

complex	$E_{1/2}\{\text{complex}\}$		$E_{1/2}\{\text{complex/pyridine}\}$		
	$E_{1/2}(1)$	$E_{1/2}(2)$	$E_{1/2}(1)$	$E_{1/2}(2)$	$E_{1/2}(3)$
$[\text{FeL}^{\text{H}}]_2$	-0.288		-1.055	-0.593	-0.160
$[\text{FeL}^{\text{Me}}]_2$	-1.013	-0.930 <sup>b</sup>	-0.732		
$[\text{FeL}^{\text{tBu}}(\text{THF})]$	-1.008		-1.095		
$[\text{FeL}^{\text{Ph}}(\text{THF})]$	-0.825		-0.715		

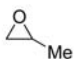
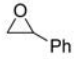

<sup>a</sup>In  $\text{CH}_2\text{Cl}_2$  at 298 K (scan rate =  $100 \text{ mV s}^{-1}$ ) using  $0.1 \text{ M NBu}_4\text{PF}_6$  as supporting electrolyte at a glassy carbon working electrode, platinum wire auxiliary electrode and Ag-AgCl (sat. NaCl) reference electrode. <sup>b</sup>Potential for irreversible reduction.

monomer-to-dimer equilibrium in catalysis as the effect (and optimization) of varying the catalyst structure and the steric bulk around the iron(III) center has not yet been established. Table 6 shows the results obtained from the catalytic cycloaddition of carbon dioxide ( $\text{CO}_2$ ) to various oxiranes providing organic carbonates (Scheme 3) using the iron(III) amino triphenolate complexes reported in this work.

When propylene oxide is studied as the substrate in dichloromethane it can be observed that the monomeric complexes are significantly more active than the dimeric complexes. When the solvent is exchanged for methylethyl ketone (MEK), which is considered to be a solvent with coordinating potential and thus can disrupt the less active dimeric structure, the use of both monomeric complexes results in good yields of carbonate. In addition to this, both the

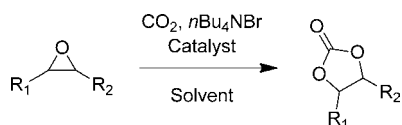


**Table 6.** Yields (%)<sup>a</sup> of Cyclic Carbonates Obtained Using [FeL<sup>H</sup>]<sub>2</sub>, [FeL<sup>Me</sup>]<sub>2</sub>, [FeL<sup>tBu</sup>(THF)], and [FeL<sup>Ph</sup>(THF)] as Catalysts for the Cycloaddition of Carbon Dioxide to Various Oxiranes

Substrate	Solvent	[FeL <sup>H</sup> ] <sub>2</sub>	[FeL <sup>Me</sup> ] <sub>2</sub>	[FeL <sup>tBu</sup> (THF)]	[FeL <sup>Ph</sup> (THF)]
	DCM	16	13	82	78
	MEK	56	72	85	88
	DCM	12	10	90	67
	DCM <sup>b</sup>	15	13	12	52
	MEK <sup>b</sup>	83	75	50	82

<sup>a</sup>Yields (%) calculated using <sup>1</sup>H NMR and mesitylene as internal standard. Conditions: 2.0 mmol epoxide, 0.01 mmol [FeL<sup>H</sup>]<sub>2</sub> and [FeL<sup>Me</sup>]<sub>2</sub> or 0.02 mmol [FeL<sup>tBu</sup>(THF)] and [FeL<sup>Ph</sup>(THF)], 0.1 mmol *n*Bu<sub>4</sub>NBr, 2.0 mmol mesitylene, 5 mL of solvent, 1.0 MPa CO<sub>2</sub>, 25 °C, 18 h. <sup>b</sup>At 85 °C. MEK = methyl ethyl ketone, DCM = dichloromethane.

### Scheme 3. Cycloaddition of Carbon Dioxide to Oxiranes to Give Cyclic Organic Carbonates



dimeric complexes now show enhanced activities, as a probable result of formation of a monomeric MEK-adduct prior to epoxide coordination and conversion. Interestingly, the use of MEK results in a slight increase in activity of [FeL<sup>Me</sup>]<sub>2</sub> over [FeL<sup>H</sup>]<sub>2</sub>, and we attribute this increase in activity to the fact that MEK is a better competitive ligand for dimer dissociation in the complex [FeL<sup>Me</sup>]<sub>2</sub> compared with [FeL<sup>H</sup>]<sub>2</sub> resulting in a more active system.

When styrene oxide is used as substrate and dichloromethane as the solvent, the monomeric complexes are again observed to be considerably more active than the dimeric complexes. [FeL<sup>Ph</sup>(THF)] is seen to be less active than [FeL<sup>tBu</sup>(THF)]. This result can be rationalized considering the accessibility of the substrate upon coordination to the iron(III) center; in the case of [FeL<sup>Ph</sup>(THF)] the substrate is relatively more embedded in the pseudocavity of the system and thus hinders the bromide for nucleophilic attack of the coordinated epoxide.

When *trans*-2,3-epoxybutane is investigated as substrate and dichloromethane as the solvent at 85 °C, poor activity is again observed for the dimeric complexes. In contrast with the previous substrates, [FeL<sup>tBu</sup>(THF)] also proves to be a poor catalyst for this substrate compared with [FeL<sup>Ph</sup>(THF)]. The difference in activities of these two monomeric complexes in dichloromethane can be rationalized by considering the steric effect of an epoxide bearing substituents on *both* carbon atoms; in this case, the steric restrictions near the coordination sphere of the metal are more dominant thus showing better performance for the less congested complex [FeL<sup>Ph</sup>(*trans*-2,3-epoxybutane)]. The steric constraints around the metal center can also be observed by looking at the increased distortion in the O–Fe–O bond angles in the solid state structure of [FeL<sup>tBu</sup>(THF)] compared with [FeL<sup>Ph</sup>(THF)]. Upon changing the solvent to MEK, all the complexes (except [FeL<sup>tBu</sup>(THF)]) display similar activities. The more sterically congested [FeL<sup>tBu</sup>(epoxide)] intermediate complex has lower activity than the other complexes as it is probably more difficult to form. Again, under these conditions (elevated temperature, coordinating medium = MEK) it appears that it has been

possible to form the more active monomeric species from [FeL<sup>H</sup>]<sub>2</sub> and [FeL<sup>Me</sup>]<sub>2</sub>.

We have been able to obtain crystals suitable for single crystal X-ray diffraction studies from [FeL<sup>Ph</sup>(THF)], whereby the tetrahydrofuran ligand is replaced by a *trans*-2,3-epoxybutane ligand (Figure 7, Table 7), indicating that the substrate is

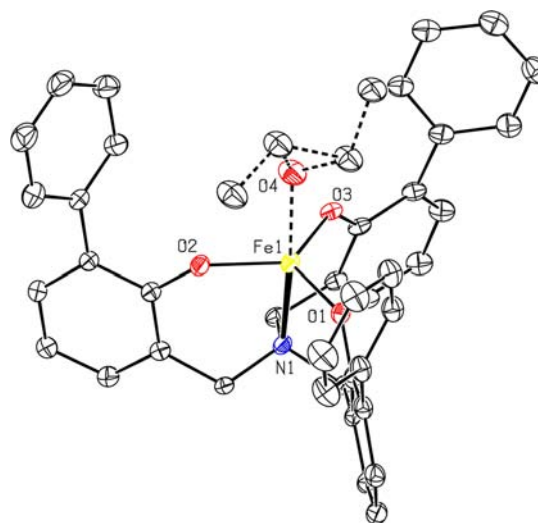


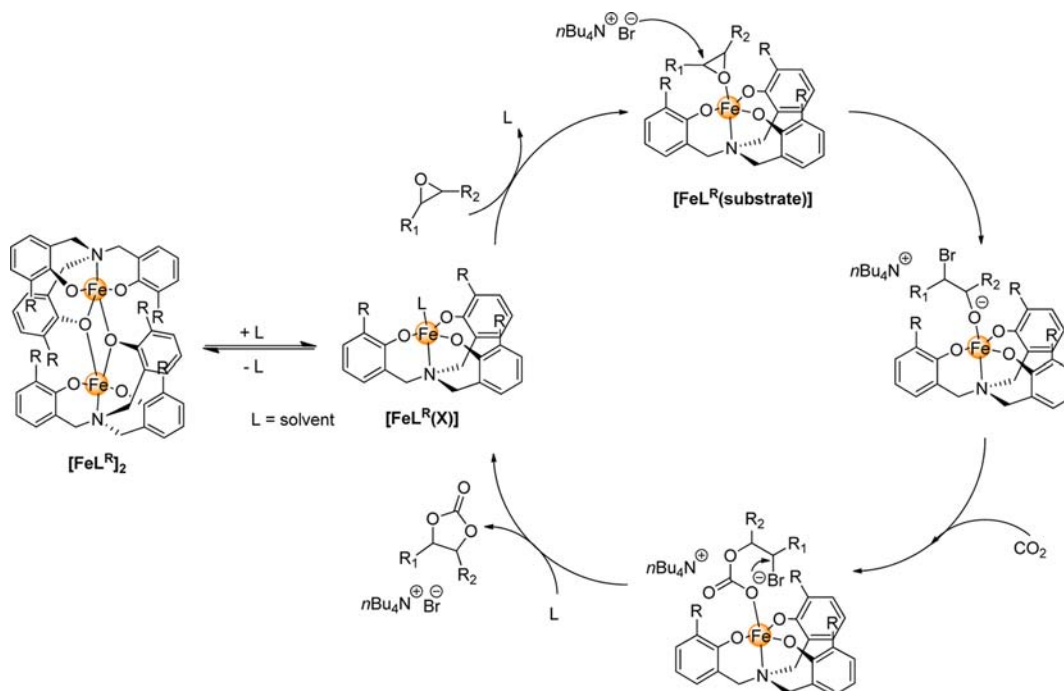
**Figure 7.** X-ray Crystal Structure of [FeL<sup>Ph</sup>(*trans*-2,3-epoxybutane)]. H-atoms, cocrystallized solvent molecules, and the disorder in the position of the epoxide ligand and the Ph groups of the ligand L are omitted for clarity. Only a partial numbering scheme is provided.

indeed able to bind to the iron(III) center. Thus, it seems that the catalytic activity of these complexes is controlled by their tendency to form dimeric structures, the solvent medium, the reaction temperature, and the steric impediment upon coordination of the substrate to the iron(III) center. Notably,

**Table 7.** Selected Bond Lengths (Å) and Angles (deg) in [FeL<sup>Ph</sup>(*trans*-2,3-epoxybutane)]

bond lengths (Å)		bond angles (deg)	
Fe(1)–O(1)	1.860(2)	O(1)–Fe(1)–O(2)	116.23(10)
Fe(1)–O(2)	1.860(2)	O(1)–Fe(1)–O(3)	119.79(10)
Fe(1)–O(3)	1.880(2)	O(1)–Fe(1)–N(1)	90.66(9)
Fe(1)–O(4)	2.145(10)	O(1)–Fe(1)–O(4)	98.00(30)
Fe(1)–N(2)	2.174(2)	O(4)–Fe(1)–N(1)	171.10(30)

Scheme 4. Proposed Mechanistic Cycle for Formation of Cyclic Organic Carbonate Products via the Monomeric Catalyst



the Fe–O<sub>epoxide</sub> distance (2.145(10) Å) is significantly longer than the Fe–O<sub>THF</sub> distance in [FeL<sup>Ph</sup>(THF)] which amounts to 2.055(5) Å, see Table 2. This may be a result of the steric requirements around the iron(III) center.

The proposed mechanistic cycle is shown in Scheme 4. It is generally accepted<sup>42–44</sup> that Lewis acid activation of the coordinated substrate is followed by ring-opening of the epoxide by the external nucleophile (here bromide) producing an iron-alkoxide intermediate. The latter reacts with CO<sub>2</sub> to form a carbonate complex through insertion of CO<sub>2</sub> into the Fe–O bond, followed by ring-closure and regeneration of the initial solvated complex.

## CONCLUSIONS

In summary, we have synthesized and fully characterized four new iron(III) amino triphenolate complexes. These complexes have been found to be dimeric (in the case of [FeL<sup>H</sup>]<sub>2</sub> and [FeL<sup>Me</sup>]<sub>2</sub>) or monomeric (in the case of [FeL<sup>tBu</sup>(THF)] and [FeL<sup>Ph</sup>(THF)]). The potential to form a dimeric structure is dependent upon the substituent in the *ortho*-position of the phenolate moiety. In the case of [FeL<sup>Me</sup>]<sub>2</sub>, though the solid state structure reveals a monomeric complex, evidence from the solution characterization methods indicates the presence of a dimer, albeit weaker in nature than the dimeric structure of [FeL<sup>H</sup>]<sub>2</sub>. Catalytic testing of the complexes for the cycloaddition of carbon dioxide to oxiranes has shown that the monomeric form of these iron complexes is significantly more active than the dimeric species. It has also been shown that by changing the reaction conditions (higher temperatures, using a solvent with coordinating potential and better CO<sub>2</sub>-dissolution potential) the dimeric structure can be disrupted and a more active form of the complex can be obtained. Our focus is now on the implementation of these iron complexes in other types of catalytic processes.

## ASSOCIATED CONTENT

### Supporting Information

Full crystallographic data in CIF format, UV–vis titration studies, and <sup>1</sup>H NMR spectra of all the complexes. This material is available free of charge via the Internet at <http://pubs.acs.org>.

## AUTHOR INFORMATION

### Corresponding Author

\*E-mail: [akleij@iciq.es](mailto:akleij@iciq.es) (A.W.K.), [giulia.licini@unipd.it](mailto:giulia.licini@unipd.it) (G.L.).

### Notes

The authors declare no competing financial interest.

## ACKNOWLEDGMENTS

We thank ICIQ, ICREA, the Spanish Ministerio de Economía y Competitividad (MINECO) through CTQ2011-27385 and COST CM1003 for support. B.G. thanks COST-D40 for a STSM at ICIQ. We also thank Prof. Miquel Costas for his helpful comments.

## REFERENCES

- (1) *Iron Catalysis in Organic Chemistry: Reactions and Applications*; Plietker, B., Ed.; Wiley-VCH: Weinheim, Germany, 2008.
- (2) Sun, C.-L.; Li, B.-J.; Shi, Z.-J. *Chem. Rev.* **2011**, *111*, 1293.
- (3) Junge, K.; Schröder, K.; Beller, M. *Chem. Commun.* **2011**, *47*, 4849.
- (4) Bolm, C.; Legros, J.; Le Paih, J.; Zani, L. *Chem. Rev.* **2004**, *104*, 6217.
- (5) *Iron-Containing Enzymes*; de Visser, S. P., Kumar, D., Eds.; RSC Publishing: Cambridge, U.K., 2011.
- (6) Fenton, H. J. H. *J. Chem. Soc.* **1894**, 65, 899.
- (7) Licini, G.; Mba, M.; Zonta, C. *Dalton Trans.* **2009**, 5265.
- (8) Tshuva, E. Y.; Goldberg, I.; Kol, M. *J. Am. Chem. Soc.* **2000**, *122*, 10706.
- (9) Hormnirun, P.; Marshall, E. L.; Gibson, V. C.; White, A. J. P.; Williams, D. J. *J. Am. Chem. Soc.* **2004**, *126*, 2688.
- (10) Egami, H.; Katsuki, T. *J. Am. Chem. Soc.* **2009**, *131*, 6082.

- (11) Yuji, S.; Kazuhiro, M.; Shoichi, K.; Hisayuki, W.; Tomoyuki, O.; Kenji, S.; Bunnai, S.; Tsutomu, K. *Angew. Chem., Int. Ed.* **2006**, *45*, 3478.
- (12) Adão, P.; Pessoa, J. C.; Henrique, R. T.; Kuznetsov, M. L.; Aveçilla, F.; Maurya, M. R.; Kumar, U.; Correia, I. *Inorg. Chem.* **2009**, *48*, 3542.
- (13) Whiteoak, C. J.; Britovsek, G. J. P.; Gibson, V. C.; White, A. J. P. *Dalton Trans.* **2009**, 2337.
- (14) Blackman, A. G. *Eur. J. Inorg. Chem.* **2008**, *17*, 2633.
- (15) Kojima, T.; Leising, R. A.; Yan, S.; Que, L., Jr. *J. Am. Chem. Soc.* **1993**, *115*, 11328.
- (16) Matsumoto, K.; Saito, B.; Katsuki, T. *Chem Commun.* **2007**, 3619.
- (17) England, J.; Britovsek, G. J. P.; Rabadia, N.; White, A. J. P. *Inorg. Chem.* **2007**, *12*, 7489.
- (18) Mayilmurugan, R.; Visvaganesan, K.; Suresh, E.; Palaniandavar, M. *Inorg. Chem.* **2009**, *48*, 8771.
- (19) Thapper, A.; Behrens, A.; Fryxelius, J.; Johansson, M. H.; Prestopino, F.; Czaun, M.; Rehder, D.; Nordlander, E. *Dalton Trans.* **2005**, *21*, 3566.
- (20) Reddig, N.; Pursche, D.; Kloskowski, M.; Slinn, C.; Baldeau, S. M.; Rompel, A. *Eur. J. Inorg. Chem.* **2004**, *4*, 879.
- (21) Wong, Y.-L.; Yan, Y.; Chan, E. S. H.; Yang, Q.; Mak, T. C. W.; Ng, D. K. P. *J. Chem. Soc., Dalton Trans.* **1998**, *18*, 3057.
- (22) van Gorkum, R.; Berding, J.; Mills, A. M.; Kooijman, H.; Tooke, D. M.; Spek, A. L.; Mutikainen, I.; Turpeinen, U.; Reedijk, J.; Bouwman, E. *Eur. J. Inorg. Chem.* **2008**, *9*, 1487.
- (23) Chmura, A. J.; Davidson, M. G.; Jones, M. D.; Lunn, M. D.; Mahon, M. F.; Johnson, A. F.; Khunkamchoo, P.; Roberts, S. L.; Wong, S. S. F. *Macromolecules* **2006**, *39*, 7250.
- (24) Blake, M. P.; Schwarz, A. D.; Mountford, P. *Organometallics* **2011**, *30* (5), 1202–1214.
- (25) Chmura, A. J.; Davidson, M. G.; Frankis, C. J.; Jones, M. D.; Lunn, M. D. *Chem. Commun.* **2008**, 1293.
- (26) Gendler, S.; Segal, S.; Goldberg, I.; Goldschmidt, Z.; Kol, M. *Inorg. Chem.* **2006**, *45*, 4783.
- (27) Kim, Y.; Jnaneshwara, G. K.; Verkade, J. G. *Inorg. Chem.* **2003**, *42*, 1437.
- (28) Mba, M.; Prins, L. J.; Licini, G. *Org. Lett.* **2007**, *9*, 21.
- (29) Mba, M.; Pontini, M.; Lovat, S.; Zonta, C.; Bernardelli, G.; Kundig, P. E.; Licini, G. *Inorg. Chem.* **2008**, *47*, 8616.
- (30) Romano, F.; Linden, A.; Mba, M.; Zonta, C.; Licini, G. *Adv. Synth. Catal.* **2010**, *352*, 2937.
- (31) Hwang, J. W.; Govindaswamy, K.; Koch, S. A. *Chem. Commun.* **1998**, 1667.
- (32) Whiteoak, C. J.; Martin, E.; Martínez Belmonte, M.; Benet-Buchholz, J.; Kleij, A. W. *Adv. Synth. Catal.* **2012**, *354*, 469.
- (33) Prins, L. J.; Mba, M.; Kolarović, A.; Licini, G. *Tetrahedron Lett.* **2006**, *47*, 2735.
- (34) Evans, D. F. *J. Chem. Soc.* **1959**, 2003.
- (35) Sur, S. K. *J. Magn. Reson.* **1989**, 169.
- (36) Sheldrick, G. M. *SHELXTL Crystallographic System*, Version 5.10; Bruker AXS, Inc.: Madison, WI, 1998.
- (37) Safaei, E.; Sheykhi, H.; Weyhermüller, T.; Eckhard, B. *Inorg. Chim. Acta* **2012**, *384*, 69.
- (38) Bartlett, R. A.; Ellison, J. J.; Power, P. P.; Shoner, S. C. *Inorg. Chem.* **1991**, *30*, 2888.
- (39) Coucouvanis, D.; Greiwe, K.; Salifoglou, A.; Challen, P.; Simopoulos, A.; Kostikas, A. *Inorg. Chem.* **1988**, *27*, 593.
- (40) Cantalupo, S. A.; Ferreira, H. E.; Bataineh, E.; King, A. J.; Petersen, M. V.; Wojtasiewicz, T.; Di Pasquale, A. G.; Rheingold, A. L.; Doerrer, L. H. *Inorg. Chem.* **2011**, *50*, 6584.
- (41) Borer, L.; Thalken, L.; Zhang, J. H.; Reiff, W. M. *Inorg. Chem.* **1983**, *22*, 3174.
- (42) Decortes, A.; Martínez Belmonte, M.; Benet-Buchholz, J.; Kleij, A. W. *Chem. Commun.* **2010**, 46, 4580.
- (43) Ema, T.; Miyazaki, Y.; Koyama, S.; Yano, Y.; Sakai, T. *Chem. Commun.* **2012**, *48*, 4489.
- (44) North, M.; Pasquale, R.; Young, C. *Green Chem.* **2010**, *12*, 1514.